JOURNAL OF AGRICULTURAL AND FOOD CHEMISTRY
ARTICLE

J. Agric. Food Chem. 2010, 58, 39–45 39
DOI:10.1021/jf902369s

Use of ATR-FTIR Microspectroscopy to Monitor Autolysis of *Saccharomyces cerevisiae* Cells in a Base Wine

Matteo Cavagna,[†] Rossana Dell'Anna,[‡] Francesca Monti,*[,§] Franca Rossi,[∥] and Sandra Torriani[†]

[†]Dipartimento di Scienze, Tecnologie e Mercati della Vite e del Vino, Università degli Studi di Verona, Via della Pieve 70, 37029 San Floriano (Verona), Italy, [‡]Fondazione Bruno Kessler−Center for Materials and Microsystems, Via Sommarive 18, 38123 Povo (Trento), Italy, [§]Dipartimento di Informatica, Università degli Studi di Verona, Strada Le Grazie 15, 37134 Verona, Italy, and [∥]Dipartimento di Biotecnologie, Università degli Studi di Verona, Strada Le Grazie 15, 37134 Verona, Italy

In this study, we evaluated the potentialities of ATR-FTIR microspectroscopy coupled to PCA in monitoring the major biochemical changes that occur during the autolysis of yeasts used for sparkling wine production. For this purpose, mid-infrared measurements were made on cells of the model strain *Saccharomyces cerevisiae* EC1118 in the course of autolysis induced at 30 °C for five days in a model and in a base wine. By relating principal component loadings to the corresponding absorption bands, it was shown that they well describe compositional modifications induced by autolytic process on yeast cells, such as partial hydrolysis of proteins, increase of peptides, free nucleotides, lipids, mannans, and β-1,3 glucans. The corresponding score−score plots allowed us to monitor the different kinetics and to distinguish among faster, intermediate, and slower processes. ATR-FTIR microspectroscopy coupled with PCA is proposed as a sensitive method that can provide useful information to select efficient yeast strains, capable of accelerated autolysis, to be used in the second fermentation and aging of sparkling wines.

KEYWORDS: Sparkling wine; yeast autolysis; FTIR microspectroscopy; ATR; PCA; biochemical changes

INTRODUCTION

The production of sparkling wines by the Champenoise or traditional method involves two fermentation steps: the first one converts must into base wine, while the second one converts base wine into sparkling wine and takes place in bottle. After the second fermentation, the yeast cells remain in contact with wine for several months in a process called aging on lees, and, during this time, autolysis of the yeasts occurs. The autolytic activities of yeasts, which follow cell death, contribute to the sensorial profile of wine with the release of flavor compounds and foaming agents. Yeast autolysis involves the degradation of cytoplasmic and cell envelope macromolecules (*1*). Well documented processes are nucleic acids hydrolysis, which gives free nucleotides and nucleosides (*2*−*4*); proteolysis, with the formation of peptides and free amino acids (*5*, *6*); and lipolysis, which releases mostly triacylglycerols and sterol esters, and also di- and monoacylglycerols, free fatty acids, sterols, and volatile compounds such as aldehydes, ketones, and esters (*7*, *8*). Last, cell wall lysis results in the release of sugars, mostly mannose, glucose, and neutral polysaccharides, such as mannans and glucomannans (*9*, *10*).

*To whom correspondence should be addressed. Dipartimento di Informatica, Università degli Studi di Verona, Strada Le Grazie 15, 37134 Verona, Italy. Tel: (+39) 045 802 7910. E-mail: francesca.monti@univr.it.

The capacity for improving flavor intensity and also for shortening the aging time depends on the ability of the yeast strain used in the second fermentation to undergo accelerated autolysis (*10*). A fast transition to autolysis is therefore an important parameter in the selection of yeast strains for sparkling wine production, and a rapid and accurate method to evaluate the autolytic capacity of wine yeasts would be extremely useful.

Most research on autolysis in oenology analyze the products released into the medium (*4*−*7*). In a previous work (*11*), we instead applied mid-infrared FTIR microspectroscopy in transmission and in ATR (attenuated total reflection) mode to the cells of the yeast strain *Saccharomyces cerevisiae* EC1118. The study was performed before and after five days of autolysis induced in a model and in a base wine. In fact, natural autolysis in wine is a slow process (many months), and laboratory induced autolysis in model systems is commonly used to accelerate it and obtain results in shorter periods of time. Through a detailed interpretation of absorption bands, obtained by curve fitting made after dividing the spectra into smaller spectral windows and with careful reference to the literature, mid-infrared FTIR microspectroscopy was shown to be an accurate technique to simultaneously probe the main biochemical modifications induced by autolysis on yeast cells as compared to other time-consuming conventional chemical and biochemical techniques (such as gas chromatography and high-performance liquid chromatography) which allow one to determine only a single family of compounds.

Published on Web 12/04/2009

Best results were obtained in the ATR mode because of its higher cell wall sensitivity and because of the fact that the most significant events which characterize autolysis involve the cell wall.

In the present study, we completed our investigation on the potentialities of ATR-FTIR microspectroscopy by monitoring the time evolution of compositional changes that occur in yeast cells during the process of autolysis together with the application of PCA (principal component analysis). Changes observed in cells can then be extrapolated to the products released in wine.

For this purpose, the autolysis of *Saccharomyces cerevisiae* EC1118, a commercial strain widely used in sparkling wine production, was induced at 30 °C for five days in a model and in a base wine following the procedure proposed by Martínez-Rodríguez et al. (*12*).

FTIR microspectroscopy measurements in ATR mode were made on samples of cells taken at different times in the course of autolysis. PCA was made on the single point spectra as well as on the average spectra at each time point in the same spectral windows where curve fitting and spectral interpretation was previously done (*11*). The meaning of the corresponding principal component loadings was explained as related to the increase or decrease of absorption bands during autolysis. The kinetics of the process was followed in the score−score plots, and allowed us to identify faster, slower, and intermediate biochemical changes, in good agreement with the literature. These are then extrapolated to what is released in wine.

MATERIALS AND METHODS

Yeast and Sample Preparation. *Saccharomyces cerevisiae* EC1118 was used in this study as a model strain for its well-known autolytic properties (*5*−*7*, *12*). An overnight culture was grown in 40 mL of YPD (yeast extract 2%, peptone 4%, and dextrose 4%) at 30 °C with shaking at 100 rpm, and cells were collected by centrifugation (8000*g*, 10 min, room temperature). Cells were washed three times with sterile physiological solution (0.9% NaCl), and suspended in 40 mL of the model wine system reported by Martinez-Rodriguez and Polo (*5*) and in 40 mL of Chardonnay base wine supplied by Cesarini Sforza SpA (Trento, Italy). The base wine had 11.2% alcohol, 0.4 g/L acetic acid, 2.2 g/L tartaric acid, and a pH of 3.2. Autolysis was induced by incubating the cell suspension at 30 °C for 5 days with shaking at 100 rpm. Samples (1 mL) were taken immediately after preparation (time 0) and after 8, 24, 72, and 120 h in the case of the model wine, and after 4, 8, 24, 48, 72, 96, and 120 h of induced autolysis in the case of the base wine. Cells were harvested by centrifugation, washed three times with sterile distilled water in order to remove wine residues, and resuspended in 500 μL of sterile water. Ten microliters of each sample was transferred to the steel supports and dried before measurements at 24 h at 40 °C to give a homogeneous cell film.

FTIR Measurements. Mid-Infrared spectra (4000−700 cm^{-1}) were acquired in ATR mode using a Vertex 70 Bruker spectrometer coupled to a Hyperion 3000 vis/IR microscope equipped with a photoconductive MCT detector and a 20× Germanium ATR-crystal objective. For each sample, i.e., for each time point, about 10 point by point spectra were recorded, by coadding 256 scans at 4 cm^{-1} (108 s of acquisition time) from a 50 μm × 50 μm area, corresponding to an estimated number of about 200 yeast cells, as the ratio of the transmitted to the incident photon intensity (I/I_0), converted into absorption spectra (ln I_0/I) and corrected for the wavelength dependence of the penetration depth inside the sample (*13*). A typical experimental spectrum is reported in **Figure 1**.

Data Analysis. Pre-processing of absorption spectra was carried out using the Bruker 5.5. OPUS software, following the procedure described by Burattini et al. (*11*). Baseline correction by the rubberband method (*13*) was made separately in the region between 3680 and 2795 cm^{-1} (named spectral window W1) and in the region between 1768 and 774 cm^{-1} to minimize introduction of artifacts due to the wavelength dependence of the background (**Figure 1**).

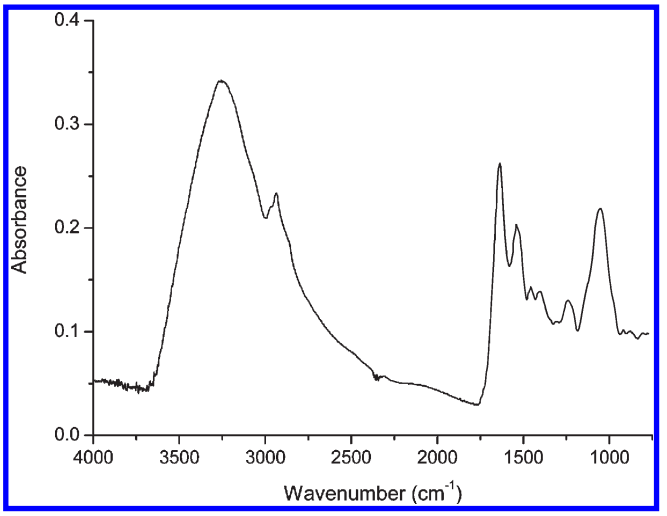

Figure 1. Typical single point experimental absorbance spectrum of *Saccharomyces cerevisiae* EC1118 between 4000 and 770 cm^{-1} at time 0 in base wine.

For each time point, an average spectrum was also obtained in each of these two main regions, by calculating the arithmetic mean of the single point baseline corrected spectra.

For subsequent analysis, the single point as well as the average spectra were further divided into the same smaller windows as in ref *11* since they were shown to be related to the main biochemical events involving contributions from specific classes of macromolecules (**Figure 2**): the W1 region was divided into two spectral windows (W1A = 3680 to 2990 cm^{-1} and W1B = 2989 to 2795 cm^{-1}), and the 1768−770 cm^{-1} region was divided into five spectral windows, 1768−1478 cm^{-1} (W2), 1478−1325 cm^{-1} (W3), 1325−1185 cm^{-1} (W4), 1185−937 cm^{-1} (W5), and 937−770 cm^{-1} (W6).

To follow the time evolution of autolysis, PCA (*14*) was applied to the single point spectra as well as to the average spectra both for the model and for the base wine in each of these spectral ranges separately, after area normalization (i.e., dividing the experimental points by the area below the curve inside each spectral window). Only for the W1B region, best results were obtained starting from the W1 area normalized spectra after a new baseline subtraction in the W1B region itself.

PCA was carried out using the available statistical packages of the R software environment (R Foundation for Statistical Computing, Vienna, Austria) after smoothing with a 11 point-Savitsky-Golay filter. Best results were obtained by mean-centering the feature vector corresponding to each spectral channel. PCA allowed us to represent the data set through score plots, which give a graphical visualization of the projections of spectra onto the principal components, PCs (*14*). As is known, each PC is a suitable linear combination of all of the original spectral components. The first principal component PC1 accounts for the maximum variance in the original data set. The second principal component PC2 is orthogonal (uncorrelated) to the first and accounts for most of the remaining variance and so on. For each spectral window, a plot of PC1 and PC2 scores was obtained, which allowed us to distinguish two groups of spectra either in PC1 or in PC2 and therefore to detect an associated time transition. In addition, the loadings of each spectral component in PC1 or PC2 were plotted and understood in terms of the increase or decrease of absorption bands, which can be related to the time transition highlighted in the score plot. Each spectral window was associated to specific biochemical processes involved in autolysis with reference to previous work (*11*) and to the literature. In this way, PCA showed different autolysis kinetics and allowed us to explain them in terms of specific and different biochemical processes.

RESULTS AND DISCUSSION

FTIR microspectroscopy in ATR mode was applied on cells of *S. cerevisiae* EC1118 sampled at different times during the process of induced autolysis in a model and in a base wine.

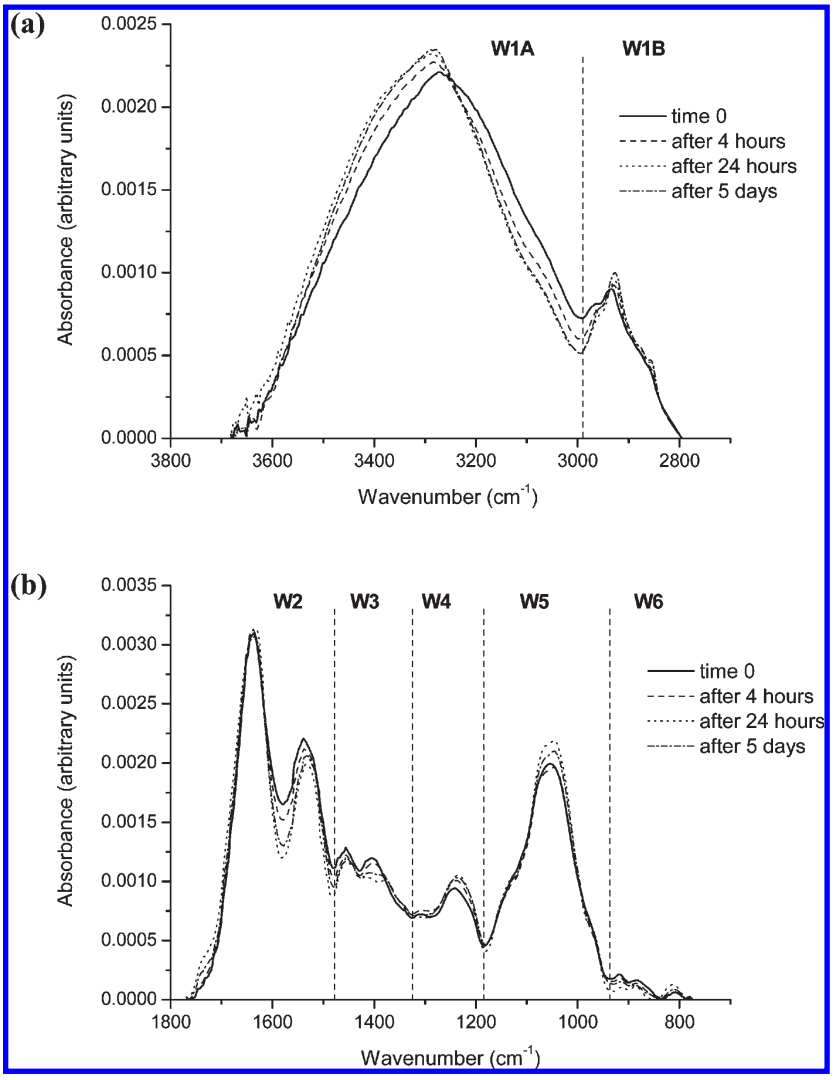

Figure 2. Average absorbance spectra (area normalized for comparison) of *Saccharomyces cerevisiae* EC1118 in base wine at time 0 and after 4 h, 24 h, and 5 days of induced autolysis. (**a**) The W1 region divided into the spectral windows W1A and W1B; (**b**) the 1768−770 cm^{-1} region divided into the five spectral windows from W2 to W6.

Saccharomyces cerevisiae EC1118 was used as a model strain since it is the most investigated in studies dealing with yeast autolysis in sparkling wine. It was shown to undergo huge cell structure modifications after 24 h of induced autolysis in a synthetic wine (*12*) and looses viability within 48−72 h (*6*, *7*), releasing higher amounts of intracellular constituents compared to those of other second fermentation yeast strains. It was also emphasized that most interesting biochemical changes involve cell envelope constituents (*15*, *16*), i.e., lipids, proteins, and polysaccharides.

FTIR microspectroscopy in ATR mode was previously proved (*11*) to be able to successfully probe global cell wall composition because of the reduced photon beam penetration depth (*13*), which in the present configuration ranges from approximately about 0.2 μm at the highest wavenumbers (spectral region W1) up to 0.8 μm at the lowest wavenumbers (spectral region W6). In addition, it was demonstrated (*2*, *12*) that the cell wall of *S. cerevisiae* maintains its integrity after cell death during incubation in model as well as in base wine, although it becomes wrinkled and ridged: this means that any change in the molecular composition of the external cell layers monitored by ATR-FTIR microspectroscopy is in turn related to an altered functionality and to the biochemistry of the autolytic process.

Average spectra in the case of the base wine in the W1 and in the 1768−770 cm^{-1} region at four representative time points (0, 4, 24, and 120 h) are shown in **Figure 2a** and **b**, respectively. The evolution of some spectral features from the time 0 sample to the autolyzed one is clearly visible.

With the aim of following the kinetics of all of the major biochemical events associated with autolysis in yeast cells, PCA was carried out both in the case of the model and of the base wine on the single point spectra as well as on the average spectra at each time point in all of the most meaningful subregions separately. The behavior of the corresponding score and loading plots is analyzed, and the obtained results are discussed in the light of previous studies (*11*), where the same spectral windows were utilized, which showed that ATR spectra are mainly sensitive to the relative increase of lipids due to membrane disorganization in W1 and W4; to the increase of mannans due to mannoprotein degradation in W4 and W5; to the break of β-1,4 and β-1,6 glucans in W5; to the transition to an unfolded state and the degradation of proteins and mannoproteins together with the relative increase in lipid content in W2 and W3; and to the increase in mannans and the hydrolysis of carbohydrates in W6.

The different kinetics were first followed in the different spectral ranges by PCA results obtained on the single point

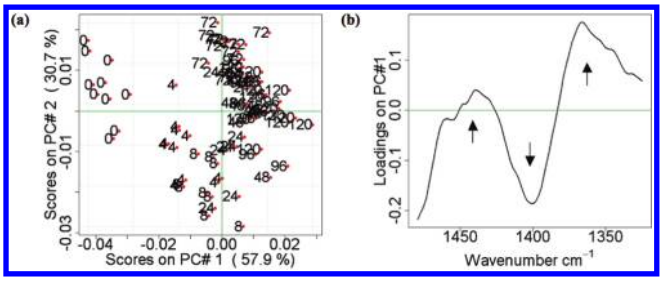

Figure 3. PC1/PC2 score−score (**a**) plot and loadings for PC1 (**b**) from PCA carried out in the W3 region on the single point spectra of *Saccharomyces cerevisiae* EC1118 in base wine from 0 to 120 h of induced autolysis. The arrows in the loading plot indicate increasing (↑) or decreasing (↓) absorption bands following the score behavior on the PC1 axis, as described in the text.

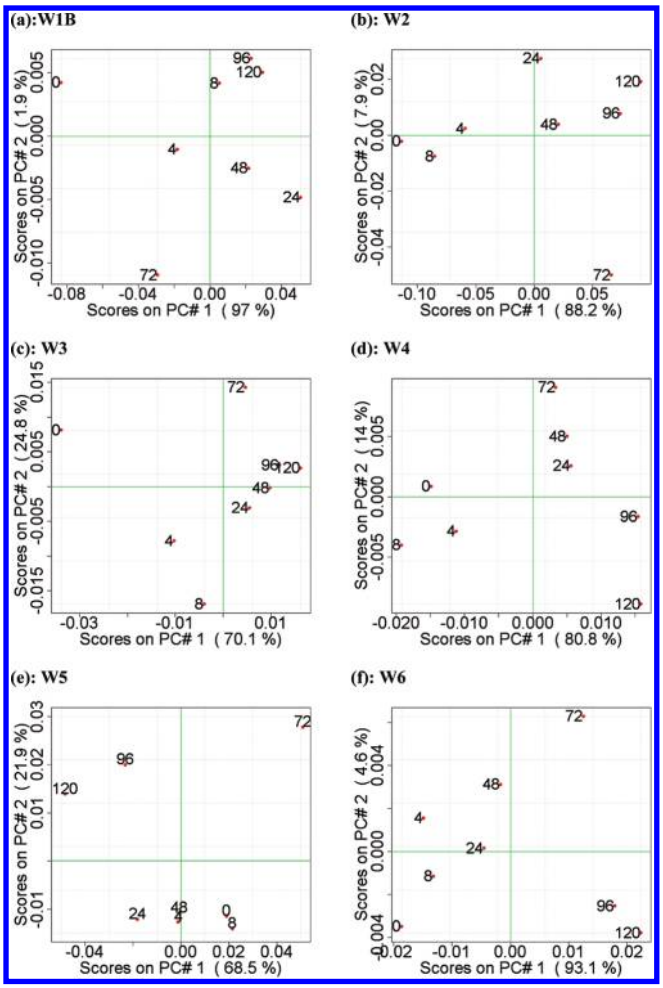

Figure 4. PC1/PC2 score−score plots from PCA carried out in the six spectral windows from W1B to W6 on the average spectra of *Saccharomyces cerevisiae* EC1118 in base wine from 0 to 120 h of induced autolysis.

spectra. The analysis was carried out on 80 spectra, and two different groups, together with an associated time transition, were visible in each subregion. **Figure 3** illustrates, as an example, the first and second principal component PC1/PC2 score−score plot together with the loadings for the first principal component PC1 in the W3 region.

To confirm the existence of the detected time transitions and to better illustrate them from a graphical point of view, the same analysis was done on the average spectra. PC1/PC2 score−score

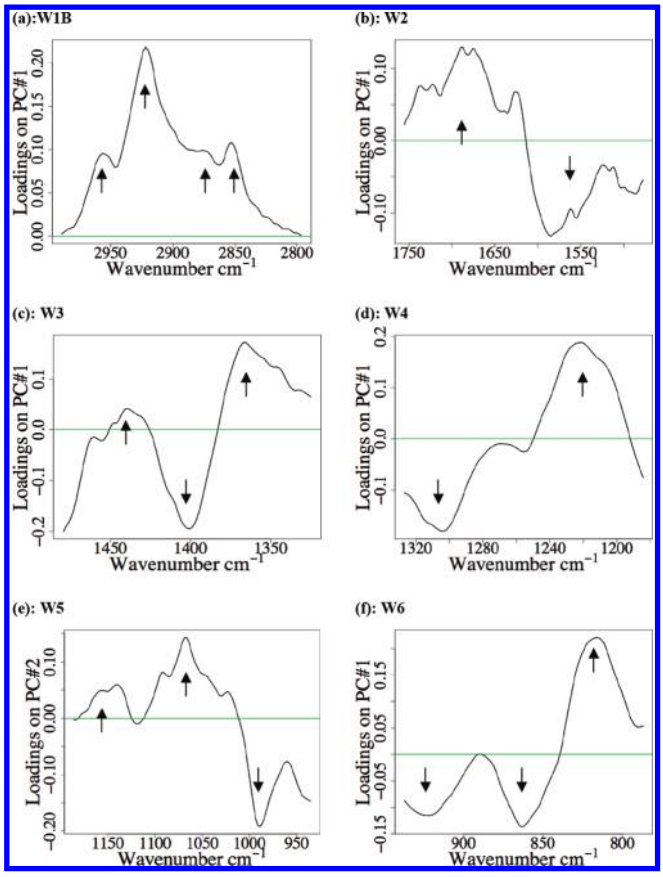

Figure 5. Loadings for PC1 (PC2 only for W5) from PCA carried out in the six spectral windows from W1B to W6 on the average spectra of *Saccharomyces cerevisiae* EC1118 in base wine from 0 to 120 h of induced autolysis. The arrows in the loading plots indicate increasing (↑) or decreasing (↓) absorption bands following the score behavior on the PC1 (PC2 only for W5) axis, as described in the text.

plots for all of the subregions from W1B to W6 are reported in **Figure 4**, while the loadings for the first principal component PC1 (the second principal component PC2 only for W5) are shown in **Figure 5**.

Scores give the projections of each spectrum onto the corresponding principal component: two groups and, consequently, a temporal transition are clearly readable in all of the score−score plots, with different time behaviors. For each spectral subregion, PC1 is the principal component sensitive to the kinetics of biochemical changes, with the only exception of W5, where, differently, the time transition is described by PC2 (**Figure 4e**). The meaning of this is that the differences between the two groups of spectra that in turn describe a time transition are associated with the variance captured by PC2. Consistently, only the loadings of PC2 are reported for W5 in **Figure 5e**.

The loadings of the principal components PC1 or PC2 allow us to relate the behavior of the score plots to the increase or decrease of absorption bands, which, in turn, is related to the biochemical processes involved in autolysis: in the spectra with positive scores, bands with positive loadings for a given PC are relatively more intense, while bands with negative loadings are relatively less intense. Vice versa, in the spectra with negative scores, bands with positive loadings are relatively less intense, while bands with negative loadings are relatively more intense. The results obtained on the average spectra strengthened those obtained on the single point ones. We also verified that the loading plots obtained in the two PCA carried the same information (compare, for example, Figures **3b** and **5c**), as expected.

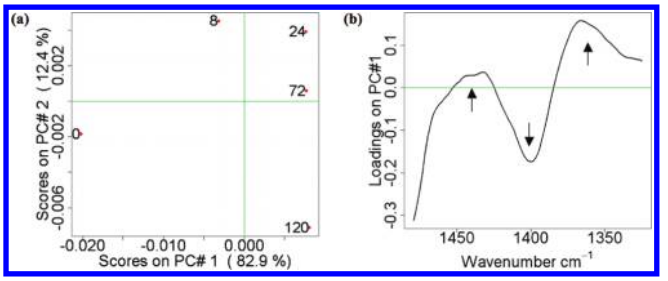

Figure 6. PC1/PC2 score−score (**a**) plot and loadings for PC1 (**b**) from PCA carried out in the W3 subregion on the average spectra of *Saccharomyces cerevisiae* EC1118 in model wine from 0 to 120 h of induced autolysis. The arrows in the loading plot indicate increasing (↑) or decreasing (↓) absorption bands following the score behavior on the PC1 axis, as described in the text.

Moreover, similar results, as regards both the score−score and the loading plots, were obtained in the case of the model wine, although samples were taken at a lower number of time points: as an example, the corresponding score−score plots and loadings are shown in **Figure 6** for the W3 subregion.

In the following, we will highlight the relationship between PCA results on the average spectra at each time and the major biochemical events involved in autolysis, consistently with the spectral interpretation summarized in **Table 1**, which was done after curve fitting and detailed comparison with the literature in Burattini et al. (ref *11* and references therein). We will show that the score−score plots allow one to monitor their different kinetics and to distinguish among faster, intermediate, and slower processes.

W1: Relative Increase of Lipids due to Membrane Disorganization. The wide and convoluted 3700−2990 cm^{-1} band (W1A) was previously shown (*11*) to be not clearly representative of some specific biochemical process involved in autolysis (**Table 1**); therefore, it was not considered in the present study. It includes the contributions of OH stretching in carbohydrates around 3400 cm^{-1}, NH stretching in proteins and peptides around 3300 and 3080 cm^{-1}, and the amide II overtone at around 3100 cm^{-1}.

The 2990−2820 cm^{-1} region (W1B) includes absorptions mainly assigned to lipids and is characterized by a more pronounced increase of CH_3 with respect to CH_2 vibrations during autolysis (*11*). Moreover, a strong reduction of the $\nu_{sym}(CH_2)/\nu_{sym}(CH_3)$ intensity ratio, which is directly proportional to the length of lipid chains, was observed after autolysis and referred to the degradation of fatty acid chains by β-oxidation. Also, the shift of the corresponding absorption bands toward higher frequencies in the autolysed samples (**Figure 2a**) can be explained by the same phenomenon.

Present PCA analysis in the W1B spectral range during autolysis is indeed sensitive to the increase in the absorption bands assigned to CH_3 and CH_2 ν_{asym} (2960 cm^{-1} and 2925 cm^{-1}) and ν_{sym} (2875 cm^{-1} and 2855 cm^{-1}) vibrations in cell wall lipids, as can be seen by the PC1 loadings reported in **Figure 5a**, and indicates that the underlying biochemical process is very fast and occurs within 4 h of induced autolysis (PC1 scores in **Figure 4a**). Since lipids are lost by the cell during autolysis (*7*), the relative increase in lipid content probably reflects their concentration in the cell remnants emptied of cytoplasmic contents and of other hydrolyzed compounds. This increase in lipid concentration with respect to other components may also come from the disorganization of the plasmatic membrane (*11*), to which ATR measurements are particularly sensitive, especially at these low wavelengths. The release of lipids from the early hours of autolysis is broadly consistent with the results obtained by Pueyo et al. (*7*). In fact, these authors observed a release of lipids over the first two days of autolysis in a model wine system with slight variations between the three commercial strains of *S. cerevisiae* considered.

Table 1. Main Absorption Bands and Assignments for the ATR-FTIR Spectra of *Saccharomyces cerevisiae* from Ref *11* and References Therein

spectral window	absorption band (cm^{-1})	main assignments
W1	∼2960	ν_{asym} CH_3 lipids
	∼2925	ν_{asym} CH_2 lipids
	∼2890	CH deformation of CH_3 lipids, proteins, and peptides
	∼2875	ν_{sym} CH_3 lipids
	∼ 2855	ν_{sym} CH_2 lipids
W2	∼1740	C═O stretching in lipid esters
	∼1670	Amide I: C═O vibrations of different protein structures
	∼1550	Amide II: N−H and C−N vibrations of the peptide bond in different protein conformations
W3	∼1470	CH_2 scissoring in lipids
	∼1455	Various CH_2/CH_3 bending vibrations in lipids and proteins
	∼1440	CH_2 deformation mainly in proteins and peptides
	∼1415	C−O−H in plane bending in proteins
	∼1405	$C(CH_3)_2$ stretching mainly in proteins
	∼1390	C═O of COO^- symmetric stretching in proteins
	∼1370	CH_2 wagging vibrations in lipids, and β-1,3 glucans
	∼1350	CH_2 wagging vibrations in lipids
	∼1340	CH_2 wagging vibrations in lipids
W4	∼1300	Amide III: C−N and C−O stretching, N−H and O═C−N bending
	∼1240	ν_{asym} PO_2^- in DNA, RNA and phospholipids
	∼1215	C−O stretching free nucleotides
	∼1200	C−O−C carbohydrates
W5	∼1156	C−O, C−OH carbohydrates, various contributions
	∼1135	mannans and β-1,3 glucans
	∼1080	ν_{sym} PO_2^- mainly from RNA
	∼1050	mannans
	∼972	mannans
	∼1108	β-1,3 glucans
	∼1025	β-1,4 glucans
	∼998	β-1,6 glucans
W6	∼915	pyranose ring asymmetric vibrations
	∼905	mannans
	∼880	β-glycosidic linkage vibrations
	∼860	α-glycosidic linkage vibrations
	∼822	mannans
	∼808	mannans
	∼780	pyranose ring symmetric vibrations, GMP ring stretching

W2: Degradation of Proteins and Mannoproteins. This region was shown (*11*) to be characterized by an increased absorption from α-form and β-sheets in the amide I zone and a decrease in the amide II band after autolysis (**Table 1**).

Present PCA analysis in this region is indeed sensitive to the same variations during the autolytic process that involve the two absorption bands at around 1670 cm^{-1} (amide I) and 1550 cm^{-1} (amide II), as can be seen by the PC1 loadings plotted in **Figure 5b**, and shows that the underlying biochemical processes occur after 8 h of induced autolysis (PC1 scores in **Figure 4b**). Increased absorptions from α-form and β-sheets in the amide I zone together with the overall decrease in the amide II band can be explained by protein and mannoprotein degradation in shorter peptides during the earlier 24 h of incubation in base wine.

This correlates well with data of timely release of nitrogen compounds in the autolysates of *S. cerevisiae* EC1118 (*5*, *6*).

W3: Membrane Disorganization and Degradation of Proteins. This region was shown (*11*) to be characterized by two wide absorption bands at around 1450 and 1400 cm^{-1}. In the former, absorptions from lipids at 1470 cm^{-1} and 1455 cm^{-1} (**Table 1**) prevailed and increased after autolysis. The second one was characterized both by the increased absorption from lipids (1350 cm^{-1}) and by a strong decrease of absorptions from proteins and mannoproteins (1400 cm^{-1}).

In this spectral range, PCA analysis during autolysis is indeed sensitive to the same variations, as can be seen by PC1 scores and loadings, plotted in **Figures 4c** and **5c**, respectively. Here, the absorption band at around 1400 cm^{-1}, related to various protein vibrations, shows an overall decrease, due to protein degradation, while the absorption bands at around 1450 and 1350 cm^{-1}, related to CH_2 wagging vibrations in lipids, show an overall increase, resulting from the disorganization of membrane systems. As a whole, PC1 scores indicate that the underlying biochemical processes occur between 4 and 8 h of induced autolysis. PCA in this region is sensitive both to plasmatic membrane disorganization and to protein degradation so that the overall kinetics shown by the score−score plot is intermediate between the two processes.

W4: Degradation of Proteins, Increase of Free Nucleotides, and Wall Polysaccharides. PCA analysis indicates that during autolysis there is an increase of an absorption band in the range 1220−1200 cm^{-1} and a decrease of an absorption band at around 1300 cm^{-1} (amide III), in agreement with previous findings, showing that this region is characterized in ATR by two absorptions at 1215 cm^{-1}, assigned to free amino acids, and at 1200 cm^{-1}, assigned to carbohydrates, which have a higher intensity after autolysis, together with the amide III absorption band, which decreased after autolysis. The underlying biochemical processes, degradation of proteins and nucleic acids, with consequent increase of free nucleotides, together with the increase of cell wall polysaccharides, occur after 8 h of autolysis (PC1 scores and PC1 loadings in **Figures 4d** and **5d**), consistently with the time behavior in W2. The general kinetics of protein and nucleic acid degradation during autolysis of *S. cerevisiae* is well documented (*4*, *5*) and shows that these processes occurred between 4 and 24 h of induced autolysis at 30 °C, in good agreement with our results. As regards polysaccharides, an early increase of these compounds in the cell wall has been previously observed by cytological staining (*8*). In addition to this, our findings also reveal a very fast kinetics of this process.

W5: Increase of Mannans and Decrease of Glucans. In this spectral range, PCA analysis during autolysis is mainly sensitive to the increase of absorption bands around 1130 cm^{-1}, 1050 cm^{-1}, and 970 cm^{-1}, previously assigned to mannans, and at around 1150 cm^{-1} (other carbohydrates), as well as to the decrease of an absorption band at around 990 cm^{-1}, which was assigned to β-1,6 glucans, and indicates that the underlying biochemical processes, increase of mannans and the hydrolysis of β-1,6 glycosidic linkages, occur only after 48 h of induced autolysis (PC2 scores in **Figure 4e** and corresponding loadings in **Figure 5e**). This confirms the relatively retarded hydrolysis of cell wall carbohydrates in the autolytic process (*1*). The increased absorption at 1080 cm^{-1}, which can also be seen in the PC2 loading, could be related to the RNA degradation resulting in an increase of free nucleotides (*3*).

W6: Increase and Hydrolysis of Mannans and Loss of Glucose Residues. In this spectral window, main absorptions were previously assigned after curve fitting to mannans, pyranose rings, and α- and β-glycosidic linkage vibrations (**Table 1**).

Main variations during the autolytic process in this region as probed by PCA are slow and occur gradually within 48 h of induced autolysis. Main changes involve absorption bands at around 920 cm^{-1} (pyranose ring) and 860 cm^{-1} (α-glycosidic linkage), which decrease probably because of the loss of glucose residues and because of the hydrolysis of mannans, and the absorption band at 820 cm^{-1} (mannans), which increases because of the rise in mannan concentration. The kinetics of these compounds is in agreement with the model of cell wall autolysis in *S. cerevisiae* proposed by Charpentier and Feuillat (*8*), which suggested a continued and slow hydrolysis of wall macromolecules starting from mannoproteins. Such degradation determines a release of mannans and hexoses over time. PCA is sensitive to a very slow process (increase of mannans) and to a relatively faster one (loss of mannose and glucose residues) so that the score−score plot behavior is intermediate between them.

To summarize, the obtained results demonstrate that mid-infrared microspectroscopy in ATR mode combined with PCA allows one to monitor three main biochemical processes involving the degradation of lipids, proteins, and polysaccharides, and to put in evidence their different kinetics: in the lipid absorption spectral window (W1B), a rapid evolution, related to the disorganization of the plasmatic membrane, is observed in the earlier 4 h of incubation; in the protein absorption region (W2), meaningful compositional modifications, related to protein and mannoprotein degradation, are observed after 8 h; in the polysaccharide region (W5), main changes, related to the increase of mannans and to the hydrolysis of β-1,6 glucans, occurs only after 48 h of induced autolysis.

This study opens the way to a new procedure for the selection of yeast strains based on their autolytic capacity by simultaneously monitoring the main biochemical events related to autolysis directly on cells. In fact, although it is presumable that strains of the same species undergo similar processes of cellular component degradation, time evolution has been shown to be strain dependent (*6*). Use of ATR-FTIR microspectroscopy, which is accurate and requires minimum sample preparation, combined with PCA, can greatly facilitate following the autolytic process kinetics of yeast starters.

ABBREVIATIONS USED

FTIR, Fourier transform infrared; ATR, attenuated total reflection; PCA, principal component analysis.

LITERATURE CITED

(1) Alexandre, H.; Guilloux-Benatier, M. Yeast autolysis in sparkling wine: a review. *Aust. J. Grape Wine Res.* **2006**, *12*, 119–127.

(2) Hernawan, T.; Fleet, G. Chemical and cytological changes during the autolysis of yeast. *J. Ind. Microbiol.* **1995**, *14*, 440–450.

(3) Zhao, J.; Fleet, G. H. Degradation of RNA during the autolysis of *Saccharomyces cerevisiae* produces predominantly ribonucleotides. *J. Ind. Microbiol. Biotechnol.* **2005**, *32*, 415–423.

(4) Charpentier, C.; Aussenac, J.; Charpentier, M.; Prome, J. C.; Duteurtre, B.; Feuillat, M. Release of nucleotides and nucleosides during yeast autolysis: kinetics and potential impact on flavor. *J. Agric. Food Chem.* **2005**, *53*, 3000–3007.

(5) Martínez-Rodríguez, A. J.; Polo, M. C. Characterization of nitrogen compounds released during yeast autolysis in a model wine system. *J. Agric. Food Chem.* **2000**, *48*, 1081–1085.

(6) Martínez-Rodríguez, A. J.; Carrascosa, A. V.; Polo, M. C. Release of nitrogen compounds to the extracellular medium by three strains of *Saccharomyces cerevisiae* during induced autolysis in a model wine system. *Int. J. Food Microbiol.* **2001**, *68*, 155–160.

(7) Pueyo, E.; Martínez-Rodríguez, A.; Polo, M. C.; Santa-María, G.; Bartolomé, B. Release of lipids during yeast autolysis in a model wine system. *J. Agric. Food Chem.* **2000**, *48*, 116–122.

(8) Charpentier, C.; Feuillat, M. Yeast Autolysis. In *Wine Microbiology and Biotechnology*; Fleet, G. H., Ed.; Harwood Academic Publishers: Lausanne, Switzerland, 1993; Chapter 7; pp 225−242.
(9) Moreno-Arribas, V.; Pueyo, E.; Nieto, F. J.; Martín-Álvarez, P. J.; Polo, M. C. Influence of the polysaccharide and the nitrogen compounds on foaming properties of sparkling wines. *Food. Chem*. **2000**, *70*, 309–317.
(10) Nunez, Y. P.; Carrascosa, A. V.; Gonzáles, R.; Polo, M. C.; Martínez-Rodríguez, A. Effect of accelerated autolysis of yeast on the composition and foaming properties of sparkling wines elaborated by a Champenoise method. *J. Agric. Food Chem*. **2005**, *53*, 7232–7237.
(11) Burattini, E.; Cavagna, M.; Dell'Anna, R.; Malvezzi Campeggi, F.; Monti, F.; Rossi, F.; Torriani., S. A FTIR microspectroscopy study of autolysis in cells of the wine yeast *Saccharomyces cerevisiae*. *Vib. Spectrosc*. **2008**, *47*, 139–147.
(12) Martínez-Rodríguez, A. J.; Polo, M. C.; Carrascosa, A. V. Structural and ultrastructural changes in yeast cells during autolysis in a model wine system and in sparkling wines. *Int. J. Food Microbiol*. **2001**, *71*, 45–51.
(13) Griffiths, P.; de Haseth, J. A. *Fourier Transform Infrared Spectrometry*; Wiley−Interscience Publishers, John Wiley & Sons: New York, 1986; p 194.
(14) Jolliffe, I. T. *Principal Component Analysis*; Springer: New York, 2002.
(15) Galichet, A.; Sockalingum, G. D.; Belarbi, A; Manfait, M. FTIR spectroscopic analysis of *Saccharomyces cerevisiae* cell walls: study of an anomalous strain exhibiting a pink-colored cell phenotype. *FEMS Microbiol. Lett*. **2001**, *197*, 179–186.
(16) Yu, C.; Irudayaraj, J. Spectroscopic characterization of microorganisms by Fourier transform infrared microspectroscopy. *Biopolymers* **2005**, *77*, 368–377.

Received for review January 20, 2009. Revised manuscript received October 29, 2009. Accepted November 1, 2009. We wish to acknowledge Fondazione CARIVERONA for its financial support.